Population characteristics, age structure, and growth dynamics of neritic juvenile green turtles in the northeastern Gulf of Mexico

Larisa Avens[1],*, Lisa R. Goshe[1], Craig A. Harms[2], Eric T. Anderson[2],
April Goodman Hall[1], Wendy M. Cluse[3], Matthew H. Godfrey[3], Joanne Braun-McNeill[1], Brian Stacy[4], Rhonda Bailey[5], Margaret M. Lamont[6]

[1]NOAA Fisheries, Southeast Fisheries Science Center, Beaufort Laboratory, 101 Pivers Island Road, Beaufort, North Carolina 28516, USA

[2]North Carolina State University College of Veterinary Medicine, Center for Marine Sciences and Technology, Morehead City, North Carolina 28557, USA

[3] North Carolina Wildlife Resources Commission, 1507 Ann St., Beaufort, North Carolina 28516, USA

[4] NOAA/National Marine Fisheries Service/Protected Resources, University of Florida, College of Veterinary Medicine, Large Animal Clinical Sciences, Gainesville, Florida 32608, USA

[5]Florida Fish and Wildlife Conservation Commission, Fish and Wildlife Research Institute, 100 8th Avenue SE, St. Petersburg, Florida 33701, USA

[6]Department of Wildlife Ecology and Conservation, University of Florida, Gainesville, Florida 32611, USA

ABSTRACT: Characterization of a population of green turtles inhabiting the northeastern Gulf of Mexico was made possible by the mortality of a subset of >4500 sea turtles that stranded during a mass cold stunning event in Florida, USA, during January 2010. In total, 434 dead, stranded green turtles *Chelonia mydas* were evaluated through necropsy and skeletochronological analysis to characterize morphology, sex, body condition, disease status, age structure, and growth patterns. Standard straightline carapace lengths ranged from 18.1 to 78.5 cm (mean ± SD = 36.3 ± 10.4 cm) and did not significantly differ from those of stranded green turtles that survived this event. Prevalence of fibropapilloma (FP) was low, at 6%, and sex ratio was significantly biased toward females (2.45F:1M). Age estimates ranged from 2 to 22 yr (mean ± SD = 9 ± 4 yr) and female age distribution was significantly greater than that of males. Mean stage durations, as calculated through summation of size class-specific growth rates and fitting smoothing spline models to length-at-age data, were similar and ranged from 17 to 20 yr. Generalized additive models and generalized additive mixed models were used to assess the potential influence of discrete and continuous covariates on growth rates. Somatic growth was significantly influenced by size, age, and calendar year; however, no effect of sex, FP status, or body condition was found. Increased understanding of population parameters will improve population models for the species and can also serve as a reference for assessing potential effects of the 2010 Deepwater Horizon oil spill in the Gulf of Mexico.

KEY WORDS: *Chelonia mydas* · St. Joseph Bay · Florida · Sea turtle · Cold stun · Skeletochronology · Sex ratio

INTRODUCTION

Effective management of threatened and endangered sea turtle species requires knowledge of not only mean values for demographic and life history parameters, but also temporal and spatial trends, the variance surrounding the means, and the underlying drivers (NRC 2010). The need for such baseline infor-

mation was recently emphasized in the aftermath of the April 20, 2010, Deepwater Horizon (DWH) MC-252 oil spill in the Gulf of Mexico during initiation of efforts to assess the effects to sea turtles of this catastrophic event (Bjorndal et al. 2011, Crowder & Heppell 2011). However, collection of these data is made difficult by deficiencies in the ability to assess sea turtle populations in an unbiased manner (Heppell et al. 2003). Population characterizations based on nesting beach studies, while prevalent due to the relative accessibility of the females on the beach, are necessarily focused in their scope (NRC 2010). In-water studies are often restricted to limited geographic areas (Bjorndal & Bolten 2000) and the proportion of individuals available to be sampled can be influenced by stage- and population-specific partitioning of habitat use (Musick & Limpus 1997, Plotkin 2003) and sex-specific behavior (Wibbels 2003). In addition, the time frames over which data collection must occur to adequately assess population parameters for these generally slow-to-mature, long-lived species are daunting (Heppell et al. 2003).

Life history data obtained from dead, stranded sea turtles can be informative, but often need to be interpreted with caution given the general lack of information regarding cause of death (natural vs. anthropogenic) (NRC 2010). The component of the population represented by stranded individuals may be influenced by biases in behavior and habitat selection (as with in-water studies), as well as the physical, environmental, and logistical factors that determine whether stranded turtles are recovered (NRC 2010). However, unusual events during which large numbers of individuals strand due to a catastrophic incident, such as mass cold-stunning (Witherington & Ehrhart 1989), can potentially provide a means for assessing a comparatively random cross-section of the affected population.

Cheloniid sea turtles are predominantly ectothermic, with body temperatures closely reflecting that of their environment (Spotila et al. 1997). As a result, water temperatures below 8 to 10°C can significantly effect sea turtle physiology; blood chemistry is altered (Anderson et al. 2011) and the turtles become lethargic and float at the water's surface, a phenomenon termed 'cold-stunning' (Milton & Lutz 2003). Mortality rates increase significantly as temperatures drop below 5 to 6°C (Schwartz 1978).

Mass cold stunning events comprising large numbers of turtles are not uncommon along the Atlantic and Gulf coasts of the USA during autumn and winter, particularly in shallow, inshore waters with restricted egress points (Foley et al. 2007, Witherington

& Ehrhart 1989). However, during January 2010, the state of Florida experienced water temperatures of 4 to 10°C for 12 d, resulting in an event of unprecedented magnitude. A total of 4613 turtles debilitated due to the cold were recovered, the majority of which were green sea turtles *Chelonia mydas* (A. Foley, FFWCC, pers. comm.). St. Joseph Bay, on Florida's northwest coast (Fig. 1), has historically been prone to cold stunning events, with the largest previously documented event comprising 401 turtles during December 2000 to January 2001 (Foley et al. 2007). During the 2010 event, this small area experienced the second highest level of cold stunning in the state, totaling 1733 turtles, with green turtles again predominating (95%) (A. Foley, FFWCC, pers. comm.). Although the majority of these turtles survived, some died due to the severity of the event.

Here we present the population characterization of 434 dead green turtles from the January 2010 St. Joseph Bay cold stun event, as evaluated through morphological characterization, necropsy, and assessment of age and growth through skeletochronological analysis of humerus bones (e.g. Zug et al. 1986, Goshe et al. 2010). Comparison of these results with data collected previously in this area provides insight into trends in population parameters. Furthermore, as green turtles comprised 17.5% of the sea turtles encountered during the response to the 2010 DWH oil spill (NOAA Fisheries OPR 2011), this information may also serve as a baseline against which to
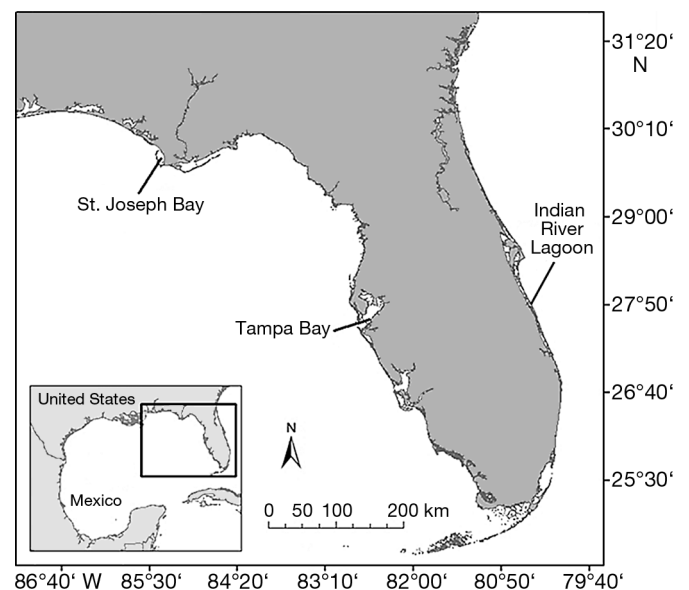

Fig. 1. Sampling sites on the coast of Florida, USA. St. Joseph Bay: origin of the cold-stunned sea turtles assessed during this study. Indian River Lagoon and Tampa Bay: other sea turtle study sites

measure potential long-term effects of this event on this species in the northeastern Gulf of Mexico.

MATERIALS AND METHODS

Population characterization and sample collection

Of the 1670 green turtles *Chelonia mydas* that cold-stunned in St. Joseph Bay, Florida, USA (Fig. 1) during January 2010, a subset of 434 of those that stranded and died between 7 and 17 January were selected for assessment and stored frozen until further evaluation was possible. Standard straightline carapace length (SCL) in centimeters (cm) (Wyneken 2001) and mass in kilograms (kg) were recorded. Each turtle then underwent a complete necropsy to determine sex through examination of the gonads, to evaluate general condition, and to document any anomalies, including tumors associated with fibropapillomatosis (FP) (Flint et al. 2009). Body condition index (BCI) was calculated as Fulton's K index (BCI = [mass/SCL^3 × 10^4]; Ricker 1975) for both the dead green turtles, as well as a subset of the surviving green turtles for which weights had been collected, to allow comparison between the 2 groups. Size, sex ratio, FP status, and body condition index data were also evaluated relative to results from previous studies conducted in this area (Foley et al. 2007, McMichael et al. 2008), as well as those from other green turtle population studies in Florida (Schroeder & Owens 1994, Kubis et al. 2009).

The humerus was extracted from the left front flipper of each turtle unless the bone was damaged, in which case the right humerus was collected instead, for use in skeletochronological analysis of age and growth (Zug et al. 1986). Each humerus was boiled to remove surrounding tissue and then allowed to dry for 2 wk prior to further processing.

Skeletochronology

A subset of humeri from 136 green turtles spanning the available size range was histologically processed for skeletochronological analysis. Samples were chosen to achieve the most comparable representation of males and females possible from all 10 cm size classes, and for size classes where >10 samples for each sex was available, humeri were randomly selected. Preparation of each humerus was conducted using the methods described in Snover & Hohn (2004) and Goshe et al. (2010). Briefly, a 2 to 3 mm thick cross-section of each humerus was first obtained using a low-speed Isomet saw (Buehler). Thick sections were decalcified using Cal-Ex II fixative/decalcifier (Fisher Scientific), and 25 μm thin sections were then taken using a freezing-stage microtome (Leica Microsystems). The thin sections were soaked overnight in Cal-Ex II and then rinsed and allowed to soak again overnight in tap water. Thin sections were stained in a 1:1 solution of water filtered through reverse osmosis and modified Ehrlich's hematoxylin stain to highlight skeletal growth marks within the tissue and then mounted on microscope slides in 100% glycerin. Partial, sequential digital images of the stained thin sections at 4× magnification were obtained using a CCD digital camera in conjunction with Microsuite image analysis software (Olympus America). The partial images were then stitched together manually using Adobe Photoshop (Adobe Systems) to yield a high-resolution, calibrated, composite digital image of the entire humerus section (e.g. Fig. 2), which was archived for later analysis.

Two independent readers (L. Avens, L. Goshe) assessed the location and number of the 'lines of arrested growth' (LAGs) that delimit the outer edges of skeletal growth marks in each humerus section (Fig. 2; Goshe et al. 2010) and worked together to

Fig. 2. *Chelonia mydas*. Stained humerus cross-section (4× magnification) from a 28.6 cm straightline carapace length (SCL) green turtle stranded dead during the January 2010 mass cold stun event in St. Joseph Bay, Florida, USA. Dotted lines denote the outer edges of skeletal growth marks, ('Lines of Arrested Growth', or LAGs). The innermost, diffuse LAG is characterized as the 'annulus' denoting the end of the first year of growth. Numbers associated with LAGs denote the calendar year during which deposition is estimated to have occurred. Age determined through skeletochronology rounded to the nearest whole year is 4 yr

reach consensus where discrepancies arose. Once consensus was reached, LAG and humerus section diameters were measured along the axis parallel to the dorsal edge of each digital section image using Microsuite Basic image analysis software. Due to the amorphous and inconsistent configurations of the resorption cores, the diameter of the innermost measurable LAG was used as a proxy for resorption core diameter during further analysis.

Age estimation

Deposition of skeletal growth marks appears to be driven primarily by endogenous, physiological cycles (Schauble 1972, Simmons 1992) synchronized with variations in environmental factors (Castanet et al. 1993). Annual deposition of skeletal growth marks has been demonstrated for known-age Kemp's ridley *Lepidochelys kempii* and loggerhead *Caretta caretta* turtles (Snover & Hohn 2004), as well as for bone-marked (Snover et al. 2011), tagged, and known-age green turtles (Goshe et al. 2010). However, due to the potential for occurrence of supplemental (non-annual) marks resulting from other factors impacting growth (Jakob et al. 2002, Snover & Hohn 2004, Olgun et al. 2005), validation of deposition frequency for each study population is preferred.

The hypothesis of annual mark deposition was tested using humeri from 3 turtles (53.6, 59.7, and 61.2 cm SCL at stranding) that had been captured, measured, and tagged a year or more prior to the cold stunning event, as done previously for loggerheads (Snover et al. 2007) and green turtles (Goshe et al. 2010) in the Atlantic. Growth marks in the humeri were examined and, assuming annual LAG deposition, a calendar year was assigned to each LAG, starting with the most recent at the external edge of the bone (e.g. Fig. 2). To allow prediction of SCL from LAG diameters, the relationship between SCL and humerus section diameter was characterized using the following allometric equation (Snover et al. 2007, Goshe et al. 2010):

$$L = L_{op} + b(D - D_{op})^c \tag{1}$$

where L is the estimated SCL, L_{op} is the minimum hatchling SCL, D is the humerus section diameter, D_{op} is the minimum hatchling humerus diameter, b is the slope of the relationship, and c is the proportionality coefficient. Values for minimum hatchling humerus diameter (2.47 mm) and SCL (4.6 cm) for green turtles in the western North Atlantic were taken from Goshe et al. (2010).

Within Eq. (1), LAG diameter was substituted for humerus section diameter, to yield an estimate of SCL at the time the LAG was formed. The body proportional hypothesis (BPH) (Francis 1990) as modified for application to sea turtles (Snover et al. 2007, their Eq. 7) was then applied to each back-calculated SCL value to yield a final SCL estimate for each LAG:

$$L_{initial} = [L_{op} + b(D_{initial} - D_{op})^c] \times \\ [L_{final}] \times [L_{op} + b(D_{final} - D_{op})^c]^{-1} \tag{2}$$

The SCL predicted for the LAG thought to be deposited closest to the time of tagging was then compared to the SCL measured at tagging using a paired sample Wilcoxon rank sum test (Zar 1996). Close correspondence between the measured and estimated SCL values would not only support correct interpretation of annual mark deposition, but also partially validate the back-calculation of annual somatic growth rates through conversion of successive LAG diameter measurements to consecutive estimates of carapace length (see 'Growth rates' section below).

Early growth marks toward the center of sea turtle bones are often lost to a phenomenon termed 'resorption', which occurs when the proportion of cancellous bone at the core expands as the turtles grow and age (Zug et al. 1986). To account for this, we used parametric and non-parametric methods to model the relationship between LAG number and LAG diameter for those humeri that retained the diffuse 'annulus' (Fig. 2) that has been characterized as marking the end of the first year of growth for Kemp's ridleys (Snover & Hohn 2004) (Group 1; n = 45, SCL mean ± SD = 29.3 ± 5.7 cm). The model with the best fit as determined by comparison of r² values was then used as a 'correction factor' (Zug & Parham 1996), to predict the number of early LAGs lost in those humeri that exhibited resorption (Group 2; n = 88, SCL mean ± SD = 50.9 ± 9.3 cm). This predicted number of lost LAGs was then added to the number of observed LAGs to yield an age estimate for each turtle. Resorption core size for 3 of the turtles (SCL mean ± SD = 70.7 ± 7.5 cm) was large enough that it fell slightly outside the range encompassed by the first correction factor. As a result, the relationship between predicted LAG number and measured LAG diameter for the humeri in Group 2 was combined with the data from Group 1, to yield a second level correction factor allowing prediction of age for these 3 individuals (Goshe et al. 2010).

Assuming a mean August or September hatch date (Hirth 1997) and late winter or spring LAG deposition as found for Kemp's ridleys (Snover & Hohn 2004),

the green turtles would have been ~x + 0.40 yr old at time of stranding when the 2010 LAG was just beginning to form (Fig. 2), but ~x + 0.75 yr old at the time of each LAG deposition. However, given that the majority of the growth is reflected in the wide growth zone and not associated with the LAGs, to simplify the growth analyses each turtle's age was rounded to the nearest whole number.

The SCL (length)-at-age data were described using a non-parametric smoothing spline model fit using the generalized cross-validation procedure to optimize the fit, while minimizing the chance of oversmoothing, and confidence intervals were generated using Bayesian posterior probabilities (Wood 2006). This relationship was then used to predict the stage duration for the size range of turtles represented in the study population.

Growth rates

Although the allometric characterization above (see 'Age estimation' section) demonstrated a positive relationship between SCL and humerus section diameter, for accurate back-calculation of growth rates a positive relationship between somatic growth and bone growth is also required (Goshe et al. 2010). To assess the association, the relationships between estimated age and SCL and estimated age and section diameter were modeled to determine which function best described the data (as determined through comparison of r^2 values). Residuals from the 2 best-fitting equations were then plotted against one another, to determine whether they were positively associated.

Assuming annual LAG deposition, calendar years were assigned to every measurable LAG visible in each humerus cross-section (e.g. Fig. 2) and, using the BPH method described above (see 'Age estimation' section), all LAG diameter measurements were converted to SCL estimates. Annual growth rates were calculated as the difference between SCL estimate pairs and each growth rate was assigned to the 10 cm size class represented by the mean of the SCL estimate pair (Chaloupka & Musick 1997). Mean, minimum, and maximum estimates of duration for the life stage represented by the study population were estimated by using size class-specific mean and mean ±1 SD growth rates to determine the length of time needed for turtles to grow through each size class and adding those estimates together.

Growth data were modeled using 2 approaches, depending on the number of growth increments from each turtle used in the analysis. A generalized additive model (GAM; Hastie & Tibshirani 1990) was applied in those cases where only 1 growth increment from each turtle could be used for analysis (equivalent to cross-sectional sampling) (Chaloupka & Musick 1997). A generalized additive mixed model (GAMM; Wood 2006) was used when multiple but varying numbers of growth increments were available for each individual (equivalent to mixed longitudinal sampling with partial replacement) (Chaloupka & Musick 1997). Both the GAM and GAMM allowed assessment of the influence of both continuous and discrete variables on growth rates and incorporated an identity link, robust quasi-likelihood error function, and cubic smoothing splines to characterize the non-linear relationship between the continuous variables and the response (growth rate) (Wood 2006). However, the GAMM made it possible to account for individual growth biases that might occur due to the mixed longitudinal sampling design, as it allowed incorporation of a turtle-specific random effect (Chaloupka & Balazs 2005). Models were implemented using the *mgcv* (GAM and GAMM) and *nlme* (GAMM) packages in the statistical program R (Wood 2006, R Development Core Team 2011). Significance of GAM and GAMM model factors was determined by *t*-ratio statistical inference (parametric covariates) and nonparametric *F*-ratio test (continuous covariates), and overall model fit was assessed using adjusted r^2 values. Further details regarding GAMs, GAMMs, and their application to sea turtle growth data, can be found in Chaloupka & Musick (1997), as well as Chaloupka & Limpus (1997).

Growth rates were divided into 4 datasets, based on the different covariates potentially associated with the growth increments. The first 2 (GAM$_{SCL}$ and GAM$_{Age}$) incorporated an individual growth rate for each turtle back-calculated from the last growth increment in each humerus (n = 136), which corresponded with the calendar year 2009. Because this was the most recent growth increment, it was possible to evaluate whether factors observed at necropsy might have contributed to growth patterns. 'SCL' and 'Age' were not incorporated into the same models, as they tend to be strongly collinear (e.g. see 'Age' section in Results), resulting in concurvity within additive models (Hastie & Tibshirani 1990) that can confound statistical inference (Ramsay et al. 2003). During preliminary GAM runs incorporating both variables, observed concurvity was high for Age and SCL (0.933 and 0.922, respectively, on a scale of 0 to 1, with 1 representing the worst-case scenario), supporting this approach. As a result, the potential

covariates for growth rate in GAM_{SCL} were Sex, SCL (cm), FP (0 = no FP, 1 = FP observed; see 'Population characteristics' section in Results), and Body Condition Index (BCI), while the potential covariates for GAM_{Age} were Sex, Age (yr), FP (0 = no FP; 1 = FP observed), and BCI.

The remaining 2 growth rate datasets ($GAMM_{SCL}$ and $GAMM_{Age}$) comprised longitudinal growth records for individual turtles back-calculated from every observed skeletal growth increment in each humerus (n = 659). Because body condition indices and incidence of FP could not be inferred beyond the recent time frame (i.e. 2009, the calendar year prior to stranding), these factors were eliminated from the GAMM analyses. Potential covariates of growth for $GAMM_{SCL}$ therefore included Calendar year, Sex, and SCL (cm), while $GAMM_{Age}$ incorporated Calendar year, Sex, and Age (yr).

RESULTS

Population characteristics

The dead green turtles ranged from 18.1 to 78.5 cm SCL (mean ± SD = 36.3 ± 10.4 cm, n = 434) (Fig. 3; Table 1). The size distribution of the dead turtles was not significantly different from that of the live-stranded green turtles from this same cold stun event (p = 0.112, Mann-Whitney *U*-test; Fig. 3).

Evaluation of gonads during necropsy using criteria outlined by Miller & Limpus (2003) demonstrated that, as expected from the size distribution, all of the turtles were immature. Sex was determined for all turtles except 3 whose internal organs had been scavenged,
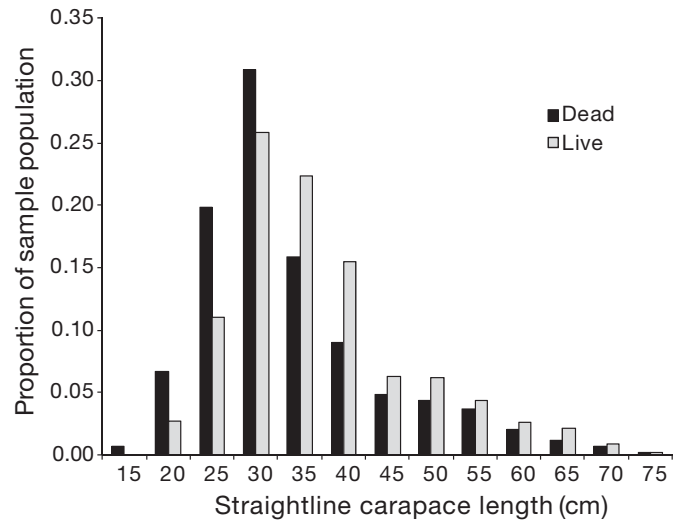

Fig. 3. *Chelonia mydas.* Proportional size distribution relative to the entire sample population for a random subset of live (n = 1190) and dead (n = 434) green turtles stranded during the January 2010 mass cold stun event in St. Joseph Bay, Florida, USA

and the sex ratio was significantly skewed toward females (2.45 F:1 M or 71% female; p < 0.0001, Pearson's chi-squared test) (Table 1). This bias toward females was less than the 3.25 F:1 M observed during the 2000–2001 St. Joseph Bay cold stun event (Table 1), but the difference was not significant (p = 0.41, Pearson's chi-squared test). Females ranged from 18.1 to 78.5 cm SCL (mean ± SD = 36.4 ± 11.1 cm) and males ranged from 21.1 to 57.9 cm SCL (36.3 ± 8.5 cm) (Fig. 4). Although all of the largest turtles in the sample were female, no significant difference was found between male and female size distributions (p = 0.328, Mann-Whitney *U*-test; Fig. 4).

External and internal examination revealed lesions ranging from major to minor, including amputations, fractures, ulcers, foreign bodies in the gastrointestinal tract, granulomas, and tissue congestion. However, due to their diversity and differing severity, full description of these lesions is outside the scope of the current study and effort was instead focused solely on characterization of fibropapillomatosis (FP). The proportion of turtles exhibiting signs of FP was low, at 6%, (Table 1) and all of these turtles exhibited only external tumors that were typically small and sparsely distributed, with <5% surface area of the soft tissues affected (e.g. Fig. 5).

Table 1. *Chelonia mydas.* Comparison of population characteristics determined for a subset of green turtles (*n* = 434) stranded dead during the 2010 cold stun event in St. Joseph Bay, Florida, with those of previous studies conducted in the same area, as well as in the Indian River Lagoon, an inshore green turtle foraging area on the east coast of Florida. SCL = straightline carapace length. [a]Foley et al. (2007), [b]McMichael et al. (2008), [c]Kubis et al. (2009), [d]Schroeder & Owens (1994)

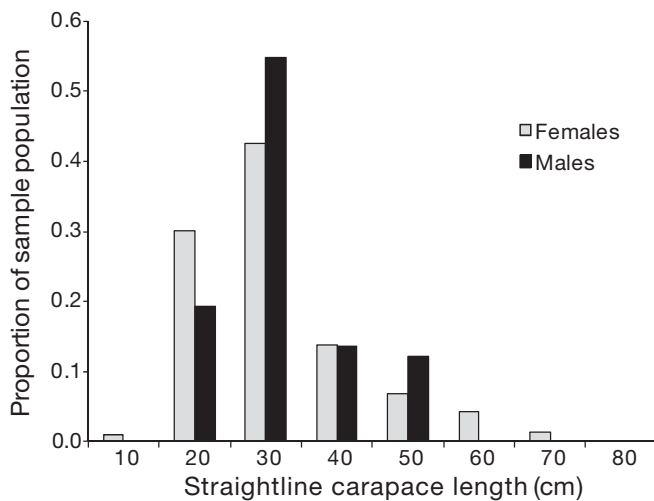| Florida inshore location	SCL (cm) Range	SCL (cm) Mean ± SD	Sex ratio (F:M)	%FP
St Joseph Bay 2010 cold stun (current study)	18.1–78.5 (n = 434)	36.3 ± 10.4	2.45:1 (n = 434)	6.00
St Joseph Bay 2000–2001 cold stun[a]	25.0–75.3 (n = 388)	36.6 ± 8.9	3.25:1 (n = 51)	0.50
St Joseph Bay 2001–2004[b]	30.9–60.8 (n = 47)	41.2 ± 6.6	–	–
Indian River Lagoon	24.3–78.6[c]	43.7 ± 10.1[c]	1.75:1[d] (n = 66)	53[c]

Fig. 4. *Chelonia mydas.* Proportional, sex-specific size distribution for dead, stranded green turtles (n = 431; females, n = 306; males, n = 125) from St. Joseph Bay, Florida, during January 2010
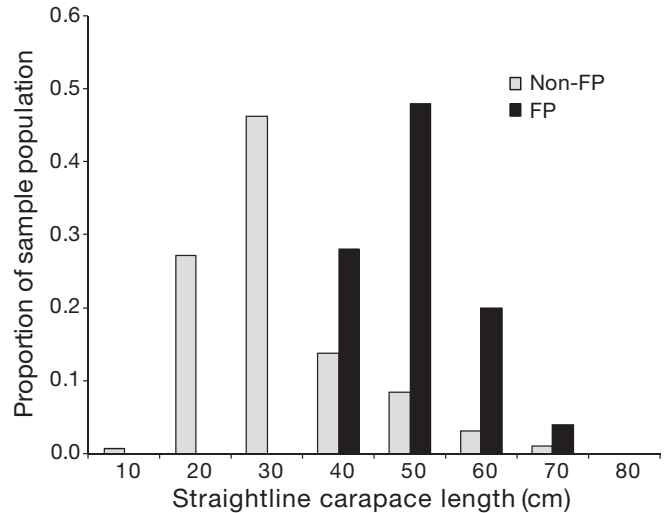

Fig. 6. *Chelonia mydas.* Proportional size distributions for dead, stranded green turtles (n = 434) exhibiting fibropapilloma (FP; n = 25) and those without (non-FP; n = 409) from St. Joseph Bay, Florida, during January 2010
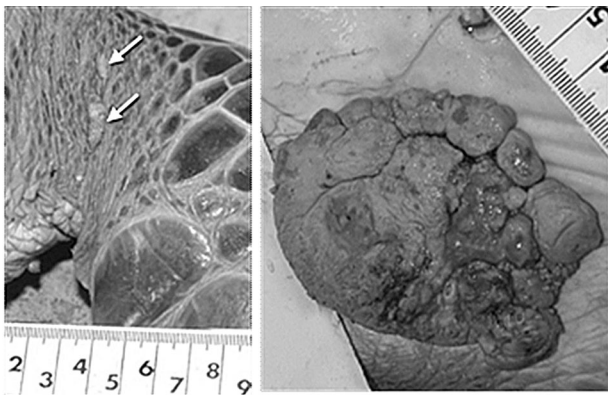

Fig. 5. *Chelonia mydas.* Fibropapillomatosis (FP) lesions of green turtles that died during the cold stun event in January 2010, in St. Joseph Bay, Florida. Left: white arrows denote the small, sparse lesions typical of turtles in the sample exhibiting FP. Right: one of the larger FP tumors documented during the population characterization

As a result, turtles were simply scored as 0 if no external FP tumors were found and 1 if FP tumors were observed, and these scores were incorporated into the GAM_{SCL} and GAM_{Age} models (see 'Growth rates' section above). The size range of the FP turtles was 44.9 to 78.5 cm SCL (mean ± SD = 55.6 ± 7.6 cm), which was significantly larger than that of the entire sample of dead turtles (p < 0.001, Mann-Whitney *U*-test; Fig. 6). Females with FP ranged from 44.9 to 78.5 cm SCL (56.2 ± 8.4 cm), while males with FP were 45.3 to 57.9 cm SCL (53.4 ± 4.5 cm). The prevalence of FP in turtles >44.9 cm SCL, the size of the smallest turtle in which FP lesions were observed,

was 33%. The sex ratio of the FP turtles was slightly, but not significantly, more biased toward females than the population as a whole (3.17 F:1 M or 76% female; p = 0.57, Pearson's chi-squared test).

Due to scavenging of internal organs, which compromised weight measurements, BCI could not be calculated for 6 of the necropsied green turtles from the 2010 cold stun event. BCI for the remaining 428 necropsied turtles ranged from 0.23 to 1.74 (mean ± SD = 1.15 ± 0.14; Table 2) and increased slightly, but significantly, with SCL (p < 0.001, r^2 = 0.053, n = 428). The difference between female and male BCIs was significant (p = 0.044; Mann-Whitney *U*-test), with females having slightly higher values than males. FP turtle BCIs ranged from 1.10 to 1.38 (1.26 ± 0.08) and were slightly higher overall, but not significantly different, than those for non-FP turtles of the same size range (BCI = 0.55 to 1.47; 1.21 ± 0.13) (p = 0.062; Mann-Whitney *U*-test). The BCIs for the dead green turtles from the 2010 cold stun were significantly greater than those for the green turtles that survived the event (p < 0.001, Mann-Whitney *U*-test; Table 2), but less than those calculated for live green turtles in St. Joseph Bay from 2001 to 2004 (Table 2).

Age

For the 3 tagged green turtles, back-calculated SCLs for the LAGs predicted to have been deposited closest to the time of original tagging were not significantly different from SCLs measured at tagging

(Table 3; p > 0.50, Wilcoxon rank sum test). Because determination of which LAG represented time at tagging was premised on the assumption of annual mark deposition, the lack of a significant difference supports this assumption and also partially validates the back-calculation of SCLs from LAG diameters for growth rate estimation (see 'Growth rates' section below).

Histological processing of all humeri selected for skeletochronology was successful, allowing analysis of each of the 136 samples, representing turtles 18.1 to 78.5 cm SCL (mean ± SD = 44.2 ± 13.7 cm). Age was estimated directly for 46 sections (Group 1) that retained all or a portion of a diffuse LAG that resembled the annulus denoting the end of the first year of growth for Kemp's ridley sea turtles (our Fig. 2; Snover & Hohn 2004). The relationship between LAG number and LAG diameter was best represented by a linear regression (Fig. 7a):

$$\text{LAG diameter} = 1.25(\text{LAG number}) + 6.55 \quad (3)$$
$$(r^2 = 0.68)$$

This equation was then used to predict the number of lost LAGs for 87 sections (Group 2) that exhibited different amounts of resorption, by substituting resorption core diameter for LAG diameter in Eq. (3). Age was estimated by adding the number of predicted LAGs to the number of observed LAGs; this exercise also allowed LAG numbers to be assigned to the observed LAGs remaining in the humeri. As resorption core diameter for 3 turtles exceeded the first correction factor, a second order correction factor was developed by combining the predicted LAG numbers and diameters for the LAGs retained in the humeri for Group 2 with the observed LAG number and diameter data from Group 1. The collective data were best characterized by a 3rd order polynomial, where x represents LAG number (Fig. 7b):

Table 2. *Chelonia mydas*. Comparison of size class-specific body condition index (BCI; mean ± SD) calculated as Fulton's K (BCI = [mass/SCL^3 × 10^4]) for dead and live green turtles from the 2010 cold stun event in St. Joseph Bay, Florida, and live green turtles assessed from 2001 to 2004 in the same study area. –: no data. [a]McMichael et al. (2008)

Size class (cm)	Dead 2010 BCI	n	Live 2010 BCI	n	Live 2001 to 2004[a] BCI	n
15–19.9	1.02 ± 0.33	3	–	–	–	–
20–29.9	1.13 ± 0.17	110	1.18 ± 0.13	97	–	–
30–39.9	1.18 ± 0.13	202	1.14 ± 0.09	397	1.35 ± 0.22	25
40–49.9	1.17 ± 0.12	60	1.14 ± 0.08	194	1.29 ± 0.17	17
50–59.9	1.23 ± 0.08	35	1.20 ± 0.07	54	1.29 ± 0.08	4
60–69.9	1.25 ± 0.12	14	1.18 ± 0.09	11	1.21	1
70–79.9	1.32 ± 0.07	4	–	–	–	–
All	1.19 ± 0.10	428	1.17 ± 0.03	753	1.29 ± 0.06	47

$$\text{LAG diameter} = -0.0015x^3 + 0.0614x^2 + 0.6914x + 7.3246 \quad (4)$$
$$(r^2 = 0.94)$$

Age for the remaining 3 turtles was estimated by substituting resorption core diameter for LAG diameter in Eq. (4) and then adding the predicted number of lost LAGs to the number of observed LAGs. Age estimates for the 136 turtles ranged from 2 to 22 yr (mean ± SD = 9 ± 4 yr; Fig. 8a), and a significant difference was found between age distributions for

Table 3. *Chelonia mydas*. Straightline carapace lengths (SCL; cm) measured at initial tagging and back-calculated through skeletochronological analysis for 3 tagged green turtles stranded dead during the 2010 cold stun event in St. Joseph Bay, Florida

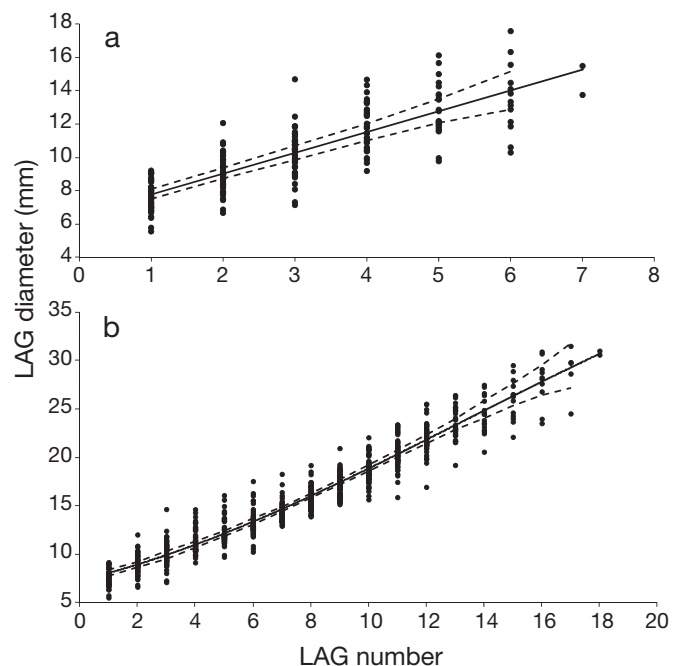| Turtle ID	Measured	Estimated	Difference
Cm072	34.0	36.1	2.1
NME20100114_009	34.7	36.0	1.3
NME20100111_042	30.8	30.1	−0.7
			Mean = 1.4

Fig. 7. *Chelonia mydas*. Relationships between line of arrested growth (LAG) number and LAG diameters for (a) Group 1 and (b) Group 1 + Group 2 (see 'Age' section in 'Results' for details regarding group characteristics, equations, and statistics). Dashed lines denote 95% CI
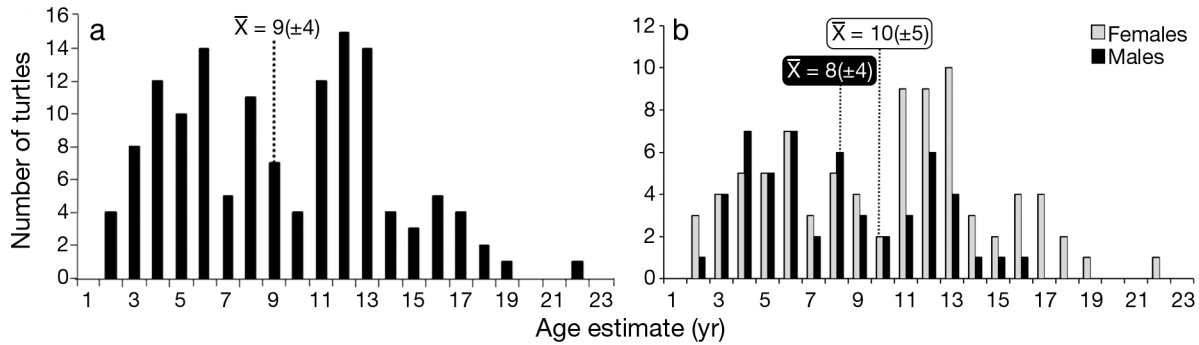
Fig. 8. *Chelonia mydas.* (a) Overall and (b) sex-specific age distributions for a subset of the dead, stranded green turtles (n = 136; females, n = 83; males, n = 53) from St. Joseph Bay, Florida, during January 2010

females (10 ± 5 yr,) and males (8 ± 4 yr) (p = 0.003, Mann-Whitney *U*-test; Fig. 8b).

A smoothing spline model was fit to both (1) the observed length-at-age data (n = 136; Fig. 9a) and (2) the length-at-age data back-calculated through conversion of all measurable LAG diameters to estimates of SCL (n = 659; Fig. 9b). As FP status was not found to influence growth rates (see 'Growth rates' below), length-at-age data from FP turtles were included in the overall analysis. SCL and age were strongly

related for Model 1 (p < 0.001, adjusted r^2 = 0.92), which predicted an age of 2 yr at 20 cm SCL, 19 to 21 yr at 78.5 cm SCL, and a total estimate of 17 to 19 yr for the turtles to grow through this size range. Model 2 yielded similar results (p < 0.001, adjusted r^2 = 0.91), with turtles 20 cm SCL estimated to be 1 yr of age and turtles 78.5 cm SCL ranging from 19 to 21 yr, producing a stage duration estimate of 18 to 20 yr. Sex-specific length-at-age relationships for both datasets were quite similar, diverging between 50
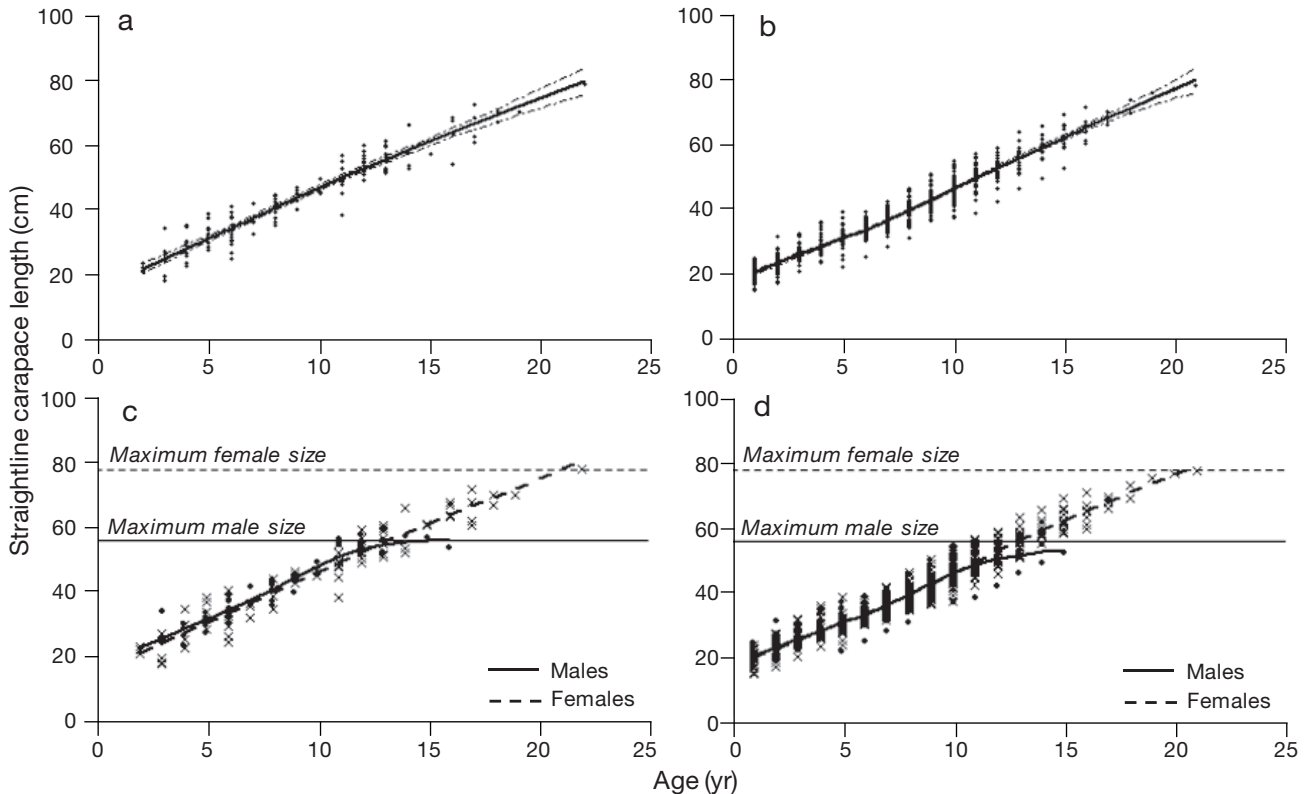

Fig. 9. *Chelonia mydas.* Smoothing spline models fit to (a) final length-at-age data (n = 136), (b) back-calculated length-at-age data for all skeletal growth marks retained in the humeri (n = 659), (c) sex-specific, final length-at-age data (females, n = 83; males, n = 53), and (d) sex-specific back-calculated length-at-age data for all skeletal growth marks retained in the humeri (females, n = 430; males, n = 229). Horizontal lines in (c) and (d) represent the maximum sizes of juvenile females and males observed in the current study

and 60 cm SCL due to the absence of males >58 cm SCL in the sample (Fig. 9c,d).

Growth rates

Both the relationship between estimated age (Age) and SCL and that for Age and humerus section diameter (HSD) were best described by 2nd order polynomials:

$$SCL = -0.03(Age)^2 + 3.54(Age) + 16.04 \quad (r^2 = 0.92) \tag{5}$$

$$HSD = -0.04(Age)^2 + 2.05(Age) + 2.38 \quad (r^2 = 0.89) \tag{6}$$

The relationship between the residuals from these 2 models was positive and best characterized by a linear regression, validating back-calculation of somatic growth rates from bone growth increments:

$$Residual\ HSD = 0.41(Residual\ SCL) + 2.35 \quad (r^2 = 0.71) \tag{7}$$

As described by Eq. (1), the relationship between SCL and HSD was allometric, with $b = 3.143895$ and $c = 0.910498$; residuals were not significantly correlated with SCL ($p = 0.170$; $r^2 = 0.0153$).

Back-calculated estimates of mean somatic growth rates per size class ranged from 2.6 to 4.0 cm SCL yr^{-1}, increasing through the 40 to 49.9 cm SCL size class and subsequently decreasing (Fig. 10a, Table 4). Mean estimate of stage duration based on size class-specific growth rates was 19.4 yr, with a minimum (mean + 1 SD) of 13.7 yr and a maximum (mean − 1 SD) of 35.0 yr (Table 4).

Growth rates relative to both SCL and Age were highly variable among individuals (Fig. 10a,b) as well as within individuals of all sizes from year to year (e.g. Fig. 10c). Retention of early LAGs was sufficient to assess trends in size class-specific mean growth rates for much of the past decade (2000 to 2009), with data for the 30.0 to 39.9 cm size class extending back to 1998 (Fig. 10a; Table 5). No consistent pattern in growth rate trends relative to calendar year was apparent among all size classes (Fig. 11a). However, the size classes (SCL) best represented in the study population (20.0–29.9 cm, 30.0–39.9 cm, 40.0–49.9 cm; Fig. 3) exhibited quite similar year-specific increases and decreases in growth rates. The observed differences in mean size class-specific
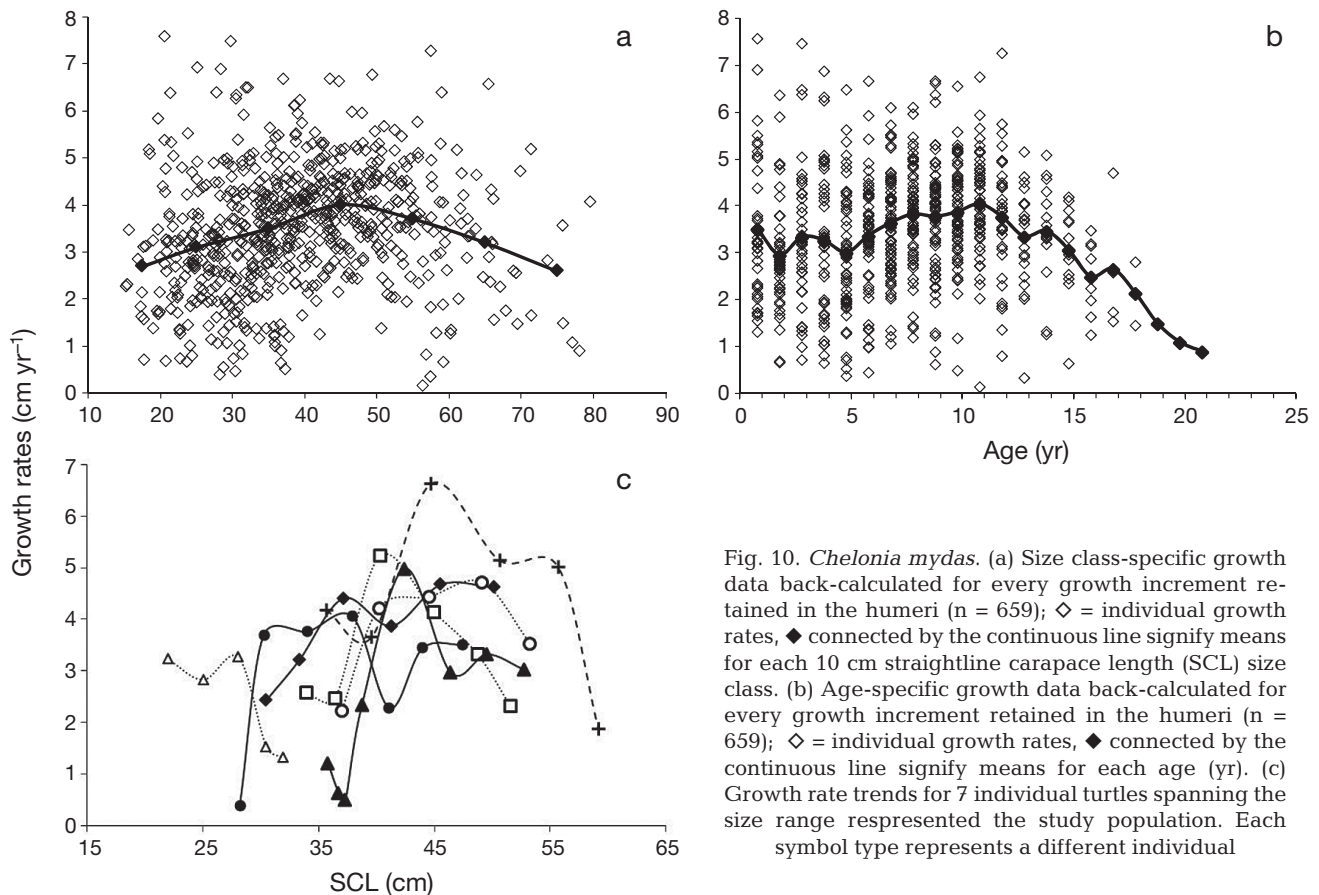

Fig. 10. *Chelonia mydas.* (a) Size class-specific growth data back-calculated for every growth increment retained in the humeri (n = 659); ◇ = individual growth rates, ◆ connected by the continuous line signify means for each 10 cm straightline carapace length (SCL) size class. (b) Age-specific growth data back-calculated for every growth increment retained in the humeri (n = 659); ◇ = individual growth rates, ◆ connected by the continuous line signify means for each age (yr). (c) Growth rate trends for 7 individual turtles spanning the size range respresented the study population. Each symbol type represents a different individual

Table 4. *Chelonia mydas*. Size class-specific straightline carapace length (SCL) growth rates back-calculated from all skeletal growth increments (n = 659) retained in the humeri of a representative sub-set of the green turtles (n = 136) stranded dead during the 2010 cold stun event in St. Joseph Bay, Florida

Size class (cm)	n	Growth rate (cm yr^{-1})		Assuming constant growth rate		
		Mean ± SD	Range	Mean	Mean −1 SD	Mean +1 SD
15–19.9	22	2.7 ±1.3	0.7–5.8	1.8	3.5	1.2
20–29.9	145	3.1 ±1.4	0.4–7.6	3.2	5.8	2.2
30–39.9	207	3.5 ±1.3	0.5–6.7	2.8	4.5	2.1
40–49.9	158	4.0 ±1.0	1.3–6.8	2.5	3.3	2.0
50–59.9	89	3.7 ±1.3	0.2–7.3	2.7	4.1	2.0
60–69.9	30	3.2 ±1.3	1.3–6.6	3.1	5.2	2.2
70–79.9	8	2.6 ±1.6	0.9–5.2	3.3	8.5	2.0
Total estimated stage duration (yr)				19.4	35.0	13.6

growth rates grouped across years (Fig. 9a, Table 4) also manifested among calendar years for the time span encompassed by this study (Fig. 11b).

Statistical and graphical outputs for the GAMs and GAMMs are summarized in Table 6 and Fig. S1 in the supplement at www.int-res.com/articles/suppl/m458p213_supp.pdf. SCL and Age were each significant predictors of growth response in the GAMs and GAMMs (Fig. S1a,e,i,l; p < 0.001 in all cases except for Age in GAM$_{Age}$, where p = 0.019). Effect of calendar year was also significant in both GAMMs (Fig. S1j,m; p < 0.001), with overall growth rates decreasing from 1998 to 2001, increasing through 2006, and then stabilizing (if not slightly decreasing). However, Sex, BCI, and FP were not found to have a significant effect on growth rates in either of the GAMs (Fig. S1b–d,f,g,h) and Sex was not a significant factor in the GAMMs (Fig. S1k,n).

DISCUSSION

Population characteristics

The size range of the dead green turtles in the current study was not significantly different from that of the green turtles that survived the 2010 cold stun event in St. Joseph Bay (Fig. 3), suggesting that the dead turtles were a representative component of the overall population. Furthermore, the size distribution of this subset is comparable to that observed during the previous 2000–2001 cold stun event (Foley et al. 2007) and also during directed sampling efforts in the area from 2001 to 2004 (McMichael et al. 2008) encompassing solely neritic stage juveniles (Table 1). However, the 2010 sample contained a greater number of small individuals that decreased the overall mean, as well as a few large turtles beyond the upper limit of the size ranges observed previously. In the western North Atlantic, green turtles typically recruit to inshore areas from oceanic developmental habitat at a size >20 cm SCL and more often at >25 cm SCL (Hirth 1997), and individuals <25 cm SCL were not present in other studies in St. Joseph Bay (Foley et al. 2007, McMichael et al. 2008). Therefore, the occurrence of 27 individuals <25 cm and 3 that were <20 cm (18.1, 18.2, and 19.7) among the dead 2010 cold stuns (Fig. 3) is somewhat unusual. Further monitoring may reveal whether this is an anomaly, or perhaps indicative of

Table 5. *Chelonia mydas*. Size class- and calendar year-specific growth rates (means ± SD; cm yr^{-1}) back-calculated from all skeletal growth increments (n = 659) retained in the humeri of a representative sub-set of the green turtles (n = 136) stranded dead during the 2010 cold stun event in St. Joseph Bay, Florida. –: no data, size class = straightline carapace length (SCL, cm)

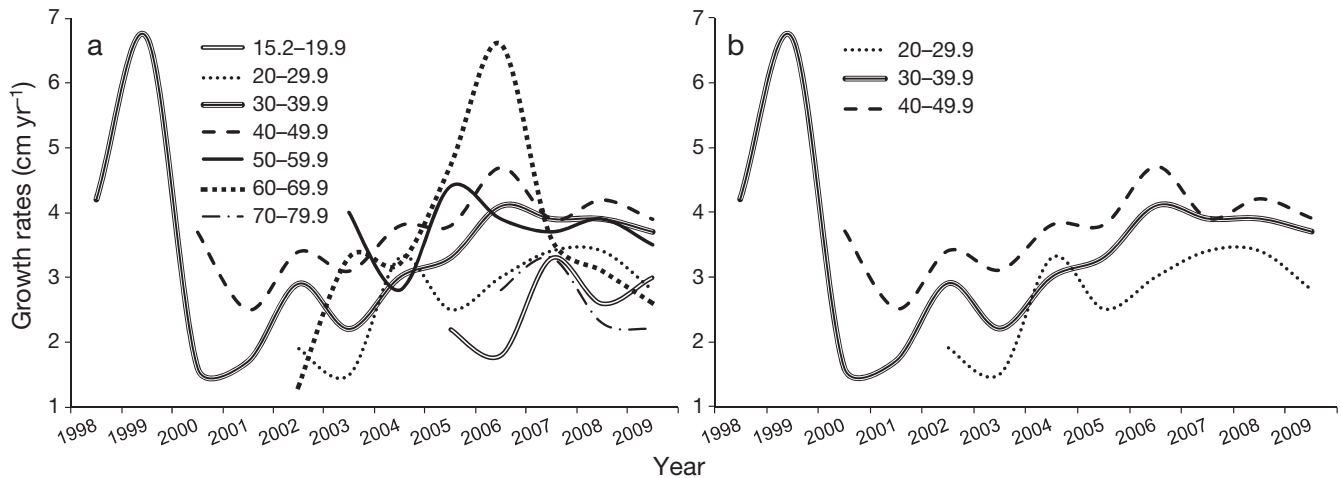| Size class: Year	15–19.9 n	Rate	20–29.9 n	Rate	30–39.9 n	Rate	40–49.9 n	Rate	50–59.9 n	Rate	60–69.9 n	Rate	70–79.9 n	Rate
1998	–	–	–	–	1	4.2	–	–	–	–	–	–	–	–
1999	–	–	–	–	1	6.7	–	–	–	–	–	–	–	–
2000	–	–	–	–	3	1.6 ± 0.3	1	3.7	–	–	–	–	–	–
2001	–	–	–	–	3	1.7 ± 0.8	2	2.5 ± 0.4	1	2.9	–	–	–	–
2002	–	–	1	1.9	8	2.9 ± 1.5	4	3.4 ± 1.3	–	–	1	1.3	–	–
2003	–	–	2	1.5 ± 1.5	8	2.2 ± 1.1	8	3.1 ± 1.0	2	4.0 ± 1.3	1	3.3	–	–
2004	–	–	4	3.3 ± 1.0	27	3.0 ± 1.2	11	3.8 ± 1.4	4	2.8 ± 1.7	1	3.2	–	–
2005	3	2.2 ± 0.8	13	2.5 ± 0.7	41	3.3 ± 0.8	11	3.8 ± 0.7	7	4.4 ± 1.8	1	4.7	–	–
2006	2	1.8 ± 0.1	32	3.0 ± 1.1	28	4.1 ± 1.0	27	4.7 ± 0.9	9	3.9 ± 1.4	1	6.6	1	2.8
2007	5	3.3 ± 1.5	34	3.4 ± 1.6	25	3.9 ± 1.0	38	3.9 ± 0.8	10	3.7 ± 1.2	3	3.6 ± 0.7	2	3.3 ± 2.6
2008	6	2.6 ± 0.8	34	3.4 ± 1.6	29	3.9 ± 1.2	34	4.2 ± 0.7	20	3.9 ± 1.4	7	3.1 ± 0.9	2	2.3 ± 1.8
2009	8	3.0 ± 1.7	24	2.8 ± 1.7	34	3.7 ± 1.6	22	3.9 ± 0.9	36	3.5 ± 1.2	11	2.6 ± 1.1	3	2.2 ± 1.7

Fig. 11. *Chelonia mydas*. (a) Back-calculated growth rate trends for all size classes (straightline carapace length, cm) represented in the study population (n = 659). (b) Back-calculated growth rate trends for the size classes most represented in the study population (20.0–29.9, 30.0–39.9, 40.0–49.9 cm; n = 510)

Table 6. *Chelonia mydas*. Summary of statistical output from the generalized additive models (GAMs) and generalized additive mixed models (GAMMs) applied to analyze the influence of different potential covariates on growth response for a representative sub-set of the green turtles (n = 136) stranded dead during the 2010 cold stun event in St. Joseph Bay, Florida. The heading 'Edf' denotes the estimated degrees of freedom. SCL = straightline carapace length. BCI = body condition index

Model	Adjusted r^2	AIC	Smooth terms Variable	Edf	F	Prob(F)	Parametric coefficients Variable	Estimate	SE	t	Pr > $|t|$
GAM$_{SCL}$	24.2	453.98	SCL (cm)	8.014	3.966	<0.001	Sex	0.407	0.233	1.747	0.083
(n = 136)			BCI	1	0.152	0.698	FP	0.005	0.303	0.017	0.987
GAM$_{Age}$	11.2	464.279	Age (yr)	2.534	3.39	0.019	Sex	0.32	0.24	1.336	0.184
(n = 136)			BCI	1	0.315	0.576	FP	0.162	0.311	0.52	0.604
GAMM$_{SCL}$	17	2146.869	SCL (cm)	2.431	13.47	<0.001	Sex	0.099	0.13	0.762	0.447
(n = 659)			Year	4.13	11.04	<0.001					
GAMM$_{Age}$	14.7	2121.759	Age (yr)	4.399	14.52	<0.001	Sex	0.055	0.134	0.41	0.682
(n = 659)			Year	4.519	11.35	<0.001					

a trend toward earlier recruitment to neritic habitat at a smaller size in this region.

All marine turtles, including green turtles, exhibit temperature dependent sexual differentiation, with warmer incubation temperatures producing greater proportions of females and cooler temperatures yielding a greater proportion of males, which creates the potential for variable sex ratios (Wibbels 2003). Sex ratio observed during this necropsy effort, as well as during the 2000–2001 St. Joseph Bay cold stun event, was significantly biased, with females comprising 70 to 76% of the population (Table 1). Genetic analysis of samples collected during the 2000–2001 event indicated that the majority (81%) of green turtles in St. Joseph Bay originated from nesting beaches in Florida and the Yucatan Peninsula in Mexico, with the remainder from Tortuguero, Costa Rica (Foley et al. 2007). Although primary sex ratio data are not available for Florida and the Yucatan, the proportion of fe-

male hatchlings estimated for Tortuguero has ranged from 67% in 1980 (Spotila et al. 1987) to 10% in 1986 and was 41% in 1988 (Horikoshi 1992). However, given that annual variation in hatchling sex ratios within and among different rookeries is likely and that the sex ratio values for foraging populations represent an integration of cohorts, it is difficult to compare values for hatchlings to those of juveniles. Neritic green turtle sex ratios (F:M) in other western North Atlantic foraging areas have not differed significantly from 1:1, with 1.75:1 during a 1989 cold stun event in the Indian River Lagoon (Schroeder & Owens 1994) and 1.4:1 in the southern Bahamas (Bolten et al. 1992). More extensive study is needed to characterize life stage- and location-specific sex ratios for green sea turtles, to allow assessment of representative values, temporal trends, and potential changes resulting from altered incubation temperatures on nesting beaches due to climate change (Hawkes et al. 2009).

Fibropapillomatosis (FP) is a tumor-forming disease most commonly found in green sea turtles, but that has also been documented in other sea turtle species (Herbst & Klein 1995). Although initial tumors are small and external, as the disease progresses debilitation and death may result because external tumors grow so large that they impede movement and foraging, and internal tumors develop that interfere with physiological function (Herbst & Klein 1995). In this study, 6% of dead green turtles exhibited small, external FP tumors that covered <5% of the surface of the soft tissues, representing an increase from the 0.5% observed for all green turtles and 0% for the dead green turtles during the 2000–2001 St. Joseph Bay cold stun (Foley et al. 2007; Table 1). However, the occurrence of the disease in this system remains far less than that observed for similarly sized green turtles in other inshore habitats in Florida, such as Tampa Bay on the west coast (53.5 to 71%; Foley et al. 2005) or the Indian River Lagoon on the east coast (61.6%; Hirama & Ehrhart 2007) (Fig. 1). The association between inshore habitat, decreased water quality due to anthropogenic impacts, and FP prevalence has long been recognized (Foley et al. 2005). Furthermore, recent modeling efforts indicate a link between increased human-induced nitrogen loading of coastal ecosystems and incidence of FP (Van Houtan et al. 2010). St. Joseph Bay is often referred to as 'one of the most pristine coastal bays in Florida' and is protected by an overlapping complement of reserves, parks, and buffer zones (Foley et al. 2007, FL DEP 2008), which may contribute to low occurrence of FP in the system. However, given the increase in FP from 2001 to 2010 and projected expansion of tourism and development in the area (FL DEP 2008), the green turtles inhabiting St. Joseph Bay should be monitored to evaluate trends in population health.

Body condition indices (BCIs) for the green turtles from the 2010 cold stun were calculated as Fulton's K index (Ricker 1975) to allow comparison with indices calculated for green turtles caught through directed sampling and stranded due to cold stunning in the same area from 2001 to 2004 (McMichael et al. 2008) (Table 2). All turtles (live and dead) from the 2010 event displayed size class-specific BCIs less than those of turtles caught during previous years, suggesting a possible decline in condition within the habitat. Comparison of dead and live green turtle BCIs from the 2010 event yielded an unexpected result; although superficially the values did not differ to a great extent, dead turtles displayed marginally but significantly higher BCIs. It is possible that the

rapid onset and severity of the cold temperatures were such that the population was affected somewhat indiscriminately relative to condition. Alternatively, it has been suggested that condition indices, such as Fulton's K, which calculate a ratio of mass to body size, are not an optimal means of characterizing condition, as the assumption of independence between the measure of condition and body size is violated (Jakob et al. 1996). Although their application fell outside the scope of the current study, other measures of condition, such as residual indices (Schulte-Hostedde et al. 2005) or scaled-mass indices (Peig & Green 2010) may prove to be more informative.

Age and growth

Although age and growth data are essential for assessing sea turtle population dynamics, this information is difficult to obtain in part due to a lack of external, age-related characteristics, along with highly migratory behavior that impedes traditional mark-recapture studies (Avens & Goshe 2007). This study represents the first skeletochronological analysis of green turtle age and growth for the Gulf of Mexico. Before the technique can be applied with confidence to generate age and growth-related information for a study population, it is necessary to: (1) validate the frequency with which LAGs are deposited in the bones, (2) characterize early LAG deposition patterns to allow estimation of the number of LAGs lost when resorption of early marks occurs, and (3) demonstrate a proportional relationship between bone growth and growth of the somatic measure of interest (Goshe et al. 2010). In the current study, analysis of humeri from 3 tagged turtles supported annual LAG deposition (Table 3). The correspondence between estimated and measured SCLs for the tagged turtles, combined with regression of the residuals from the Age-SCL and Age-Humerus Section Diameter relationships, supported the validity of back-calculating somatic growth rates from bone growth increments (see 'Growth rates' section in 'Results'). Finally, 33% of the turtles for which age was estimated retained what appeared to be an annulus (Fig. 2), which is a diffuse LAG described as denoting the end of the first year of growth (Snover & Hohn 2004), and therefore exhibited no resorption. Characterization of the relationship between LAG number and diameter for these turtles allowed development of a robust correction factor that could be used to estimate the number of resorbed LAGs in the humeri from older, larger turtles in the sample.

Although the year-specific growth response observed in the GAMMs raises the possibility that LAG-number:LAG-diameter relationships estimated prior to 1998 may deviate somewhat from the correction factors applied here, this question could not be evaluated with the available data.

The ages predicted for the subset of 136 green turtles from the 2010 cold stun spanned 2 to 22 yr and the distribution was multi-modal (Fig. 8a). Further study is needed to determine whether this result represents an anomalous sampling effect, is related to nesting cycles for the various source populations (e.g. Troëng & Rankin 2005), or is perhaps the result of differential survival of the less-represented cohorts. The significant difference between female and male age distributions (Fig. 8b) is also intriguing, as it could be indicative of changes in hatchling sex ratios on nesting beaches, differential mortality of male and female juveniles, or a combination of factors. The length-at-age relationships for males and females of comparable size classes as described by the smoothing spline models in the current study (Fig. 9c,d) were quite similar and, taken together, suggest a neritic stage duration for the juvenile green turtles inhabiting St. Joseph Bay of approximately 17 to 20 yr (Fig. 9a,b).

Evaluation of individual growth rates revealed a high level of variability relative to both SCL and age (Fig. 10a,b) as well from year to year for individuals (Fig. 10c) and size classes (Fig. 11, Table 5). Summation of mean estimated time to grow through each size class represented in the study population yielded a neritic juvenile stage duration estimate of

19.4 yr (Table 4), which was quite comparable to the results yielded by the length-at-age models (Fig. 9a,b). Standard deviations for mean growth rates were used to calculate a range of stage durations (Table 4) because individual variability in growth (e.g. Fig. 10c) indicates that it is unlikely that absolute minimum and maximum growth rates persist throughout life. Furthermore, while use of these absolute values for estimation of stage duration yielded a reasonable minimum estimate (9.8 yr, assuming ideal conditions), the maximum projection was unrealistic (127.3 yr).

Size class-specific growth rates in the current study fell within the range of growth rates reported from other areas in the western North Atlantic, with the exception of the extremely rapid growth noted for small turtles in the Indian River Lagoon (IRL), Bahamas, US Virgin Islands (USVI), and Puerto Rico (PR) (Table 7). Back-calculated growth rates in the current study spanned from 1998 to 2009 and indicated an overall peak in growth for the 40.0 to 49.9 cm SCL size class (Fig. 10a), which is a larger peak size than that observed for the IRL, Bahamas, and USVI, but smaller than that calculated for green turtles on the Atlantic coast of the USA (Table 7). Interestingly, the growth rates presented here are somewhat less than those observed by McMichael et al. (2008) for green turtles in St. Joseph Bay from 2001 to 2004 (Table 7). However, this difference might be at least partly due to averaging of growth rates over recapture intervals >1 yr in the previous study, given the significant effect of calendar year on growth observed in the GAMM analyses

Table 7. *Chelonia mydas*. Comparison of size class-specific growth rates determined through skeletochronology for a representative sub-set (n = 136) of the green sea turtles stranded dead during the 2010 cold stun event in St. Joseph Bay, Florida, with green turtle growth rates collected from other areas in the western North Atlantic using either mark-recapture or skeletochronology. SCL = straighline carapace length; IRL = Indian River Lagoon; TSB = Trident Submarine Basin; SIR = Sebastian Inlet Reef; STL = St. Lucie Power Plant Reef; USVI = US Virgin Islands. –: no data. [a]Growth rates obtained using skeletochronology, [b]Growth rates obtained through mark-recapture, [c]Sample size = 1

Area		Mean growth rate (cm yr^{-1})						
Size class (cm SCL):	15–19.9	20–29.9	30–39.9	40–49.9	50–59.9	60–69.9	70–79.9
St. Joe Bay 2010 (current study)[a]	2.7	3.1	3.5	4.0	3.7	3.2	2.6
St. Joe Bay 2001–04 (McMichael et al. 2008)[b]	–	–	4.7	4.3	4.8	3.8[c]	–
W. N. Atlantic (Goshe et al. 2010)[a]	3.3	3.0	2.1	2.5	2.7	3.3	2.4
Florida inshore (Zug & Glor 1998)[a]	–	3.1	4.4	4.8	5.3	4.1	1.3[c]
Florida inshore (IRL) (Kubis et al. 2009)[b]	–	–	3.6	4.0	4.6	4.0	2.8
Florida inshore (TSB) (Kubis et al. 2009)[b]	–	1.8	2.3	1.6	–	–	–
Florida nearshore (SIR) (Kubis et al. 2009)[b]	–	1.3	2.0	2.4	3.0	2.5	–
Florida nearshore (STL) (Kubis et al. 2009)[b]	–	1.2	2.1	2.5	2.6	2.8	–
Bahamas (Bjorndal & Bolten 1988)[b]	–	–	8.8	4.9	3.1	1.8	1.9
USVI (Boulon & Frazer 1990)[b]	–	6.9	5.0	4.7	3.5	1.9	3.9
Puerto Rico (Collazo et al. 1992)[b]	–	3.6	5.1	6.0	3.8	3.9	–

(Fig. S1j,m). Temporal and spatial distribution of sampling effort could have an influence as well, as habitat partitioning due to forage availability, experience, and predation or threat risk considerations can result in differential growth rates even within small spatial areas (Werner et al. 1981, Werner & Hall 1988, Persson 1993). The high degree of inter- and intra-individual growth rate variability observed in the current study (Fig. 10a,b) also indicates that large sample sizes are needed to comprehensively evaluate green turtle growth rates and patterns.

Previous studies have speculated that the lack of explanatory power for covariates included in additive models, such as GAMs and GAMMs, might result from the inability to fully characterize all potential growth covariates, particularly age and cohort (Chaloupka & Limpus 1997, Limpus & Chaloupka 1997). Although the 2010 cold stun represented a singular opportunity to assess a random cross-section of the green turtle population inhabiting St. Joseph Bay, the discrete nature of the dataset also limits the number of potential covariates that can be included in the models. However, the current analysis demonstrates that for green turtles inhabiting St. Joseph Bay, growth rate was less dependent upon age than size (Fig S1a,e,i,l, Table 6). For the 2009 growth interval, no significant effect was found for either BCI calculated as Fulton's K (Fig. S1b,f, Table 6) or FP status (Fig. S1d,h, Table 6). The latter finding is consistent from results of Hawaiian green turtle studies, where growth response was not influenced by FP unless symptoms were severe (Chaloupka & Balazs 2005). In contrast to other green turtle growth assessments in the Bahamas (Bjorndal et al. 2000) and Australia (Limpus & Chaloupka 1997), no significant sex-specific growth effects were found for turtles in the current study (Table 6). This result suggests that it may not be necessary to incorporate sex as a factor when modeling juvenile green sea turtle age and growth in our study area. However, the growth response was higher for males in all models except GAMM$_{Age}$ (Fig. S1c,g,k,n), and therefore the lack of significance may simply result from the absence of larger individuals from analyses (Limpus & Chaloupka 1997, Bjorndal et al. 2000). A significant temporal trend for growth response in St. Joseph Bay was observed (Fig. S1j,m), indicating that growth rates reached their lowest levels around 2001, increased through 2006, and have subsequently stabilized or even decreased to some extent. Although absolute sea turtle abundance data are not available for this area, strongly positive trends in cold stun numbers since the early 1980s allow for the possibility that turtle numbers in St. Joseph Bay may be increasing (Foley et al. 2007). If this is the case, growth trends may at least partly reflect density-dependent effects (Bjorndal et al. 2000); however, effects due to shifts in genetic composition (Bjorndal et al. 2000) or anthropogenic impacts on turtle health and habitat quality are also possible.

Conclusions and implications

Currently, sea turtle population assessment efforts are hindered by a lack of demographic, vital-rate, and life history data, particularly for in-water populations (NRC 2010). The goal of the current study was to combine necropsy and skeletochronology to comprehensively characterize the green sea turtle population inhabiting St. Joseph Bay, Florida, USA, and provide data to contribute to population models for the species. In addition to the approaches described here, understanding of the dynamics of this population could be further enhanced by genetic, stable isotope, and toxicological analyses, which would provide insight into stock structure, foraging history, and contaminant loads. Integration of diverse, complementary approaches for study of sea turtle populations over long time periods is essential for understanding the potential scope and causes of variability for population parameters (Heppell et al. 2003) as well as evaluating potentially deleterious effects of catastrophic events, such as the 2010 DWH oil spill.

LITERATURE CITED

Anderson ET, Harms CA, Stringer EM, Cluse WM (2011) Evaluation of hematology and serum biochemistry of cold-stunned green sea turtles (*Chelonia mydas*) in North Carolina, USA. J Zoo Wildl Med 42:247–255

Avens L, Goshe LR (2007) Comparative skeletochronological analysis of Kemp's ridley (*Lepidochelys kempii*) and loggerhead (*Caretta caretta*) humeri and scleral ossicles. Mar Biol 152:1309–1317

Bjorndal KA, Bolten AB (1988) Growth rates of immature green turtles, *Chelonia mydas*, on feeding grounds in the southern Bahamas. Copeia 1988:555–564

Bjorndal KA, Bolten AB (eds) (2000) Proceedings of a workshop on assessing abundance and trends for in-water sea turtle populations. US Dep Commer NOAA Tech Mem NMFS-SEFSC-445

Bjorndal KA, Bolten AB, Chaloupka MY (2000) Green turtle somatic growth model: evidence for density dependence. Ecol Appl 10:269–282

Bjorndal KA, Bowen BW, Chaloupka M, Crowder LB and others (2011) Better science needed for restoration in the Gulf of Mexico. Science 331:537–538

Bolten AB, Bjorndal KA, Grumbles JA, Owens DW (1992) Sex ratio and sex-specific growth rates of immature green turtles, *Chelonia mydas*, in the southern Bahamas. Copeia 1098–1103

Boulon RH Jr, Frazer NB (1990) Growth of wild juvenile Caribbean green turtles, *Chelonia mydas*. J Herpetol 24: 441–445

Castanet J, Francillon-Viellot H, Meunier FJ, De Ricqles A (1993) Bone and individual aging. In: Hall BK (ed) Bone. Bone growth — B, Vol 7. CRC Press, Boca Raton, FL, p 245–283

Chaloupka MY, Balazs G (2005) Modelling the effect of fibropapilloma disease on the somatic growth dynamics of Hawaiian green sea turtles. Mar Biol 147:1251–1260

Chaloupka MY, Limpus CJ (1997) Robust statistical modeling of hawksbill sea turtle growth rates (southern Great Barrier Reef). Mar Ecol Prog Ser 146:1–8

Chaloupka MY, Musick JA (1997) Age, growth, and population dynamics. In: Lutz PL, Musick JA (eds) The biology of sea turtles. CRC Press, Boca Raton, FL, p 233–276

Collazo JA, Boulon R Jr, Tallevast TL (1992) Abundance and growth patterns of *Chelonia mydas* in Culebra, Puerto Rico. J Herpetol 26:293–300

Crowder L, Heppell S (2011) The decline and rise of a sea turtle: how Kemp's ridleys are recovering in the Gulf of Mexico. Solutions 2:67–73

Flint M, Patterson-Kane JC, Limpus CJ, Work TM, Blair D, Mills PC (2009) Postmortem diagnostic investigation of disease in free-ranging marine turtle populations: a review of common pathologic findings and protocols. J Vet Diagn Invest 21:733–759

FL DEP (Florida Department of Environmental Protection) (2008) St. Joseph Bay Aquatic Preserve Management Plan — September, 2008–August, 2018. Florida Department of Environmental Protection. Accessed 11 October 2011 www.dep.state.fl.us/coastal/sites/stjoseph/pub/StJosephBay_2008.pdf

Foley AM, Schroeder BA, Redlow AE, Fick-Child KJ, Teas WG (2005) Fibropapillomatosis in stranded green turtles (*Chelonia mydas*) from the eastern United States (1980–98): trends and associations with environmental factors. J Wildl Dis 41:29–41

Foley AM, Singel KE, Dutton PH, Summers TM, Redlow AE, Lessman J (2007) Characteristics of a green turtle (*Chelonia mydas*) assemblage in northwestern Florida determined during a hypothermic stunning event. Gulf Mex Sci 2007:131–143

Francis RICC (1990) Back-calculation of fish length: a critical review. J Fish Biol 36:883–902

Goshe LR, Avens L, Scharf FS, Southwood AL (2010) Estimation of age at maturation and growth of Atlantic green turtles (*Chelonia mydas*) using skeletochronology. Mar Biol 157:1725–1740

Hastie TJ, Tibshirani RJ (1990) Generalized additive models. Monographs on statistics and applied probability, 43. Chapman & Hall, London

Hawkes LA, Broderick AC, Godfrey MH, Godley BJ (2009) Climate change and marine turtles. Endang Species Res 7:137–154

Heppell SS, Snover ML, Crowder LB (2003) Sea turtle population ecology. In: Lutz PL, Musick JA, Wyneken J (eds) The biology of sea turtles, Vol 2. CRC Press, Boca Raton, FL, p 275–306

Herbst LH, Klein PA (1995) Green turtle fibropapillomatosis: challenges to assessing the role of environmental cofactors. Environ Health Perspect 103:27–30

Hirama S, Ehrhart LM (2007) Description, prevalence and severity of green turtle fibropapillomatosis in three developmental habitats on the east coast of Florida. Fla Sci 70:435–448

Hirth HF (1997) Synopsis of the biological data on the green turtle *Chelonia mydas* (Linnaeus 1758). U. S. Fish and Wildlife Service Biological Report 97(1), Washington DC

Horikoshi K (1992) Egg survivorship and primary sex ratio of green turtles, *Chelonia mydas*, at Tortuguero, Costa Rica. PhD dissertation, University of Florida, Gainesville

Jakob EM, Marshall SD, Uetz GW (1996) Estimating fitness: a comparison of body condition indices. Oikos 77:61–67

Jakob C, Seitz A, Crivelli AJ, Miaud C (2002) Growth cycle of the marbled newt (*Triturus marmoratus*) in the Mediterranean region assessed by skeletochronology. Amphib-Reptilia 23:407–418

Kubis S, Chaloupka M, Ehrhart L, Bresette M (2009) Growth rates of juvenile green turtles *Chelonia mydas* from three ecologically distinct foraging habitats along the east central coast of Florida, USA. Mar Ecol Prog Ser 389: 257–269

Limpus C, Chaloupka M (1997) Nonparametric regression modeling of green sea turtle growth rates (southern Great Barrier Reef). Mar Ecol Prog Ser 149:23–34

McMichael E, Seminoff J, Carthy R (2008) Growth rates of wild green turtle, *Chelonia mydas*, at a temperate foraging habitat in the northern Gulf of Mexico: assessing short-term effects of cold-stunning on growth. J Nat Hist 42:2793–2807

Miller JD, Limpus CJ (2003) Ontogeny of marine turtle gonads. In: Lutz PL, Musick JA, Wyneken J (eds) The biology of sea turtles, Vol 2. CRC Press, Boca Raton, FL, p 199–224

Milton SL, Lutz PL (2003) Physiological and genetic responses to environmental stress. In: Lutz PL, Musick JA, Wyneken J (eds) The biology of sea turtles, Vol 2. CRC Press, Boca Raton, FL, p 163–197

Musick JA, Limpus CJ (1997) Habitat utilization and migration in juvenile sea turtles. In: Lutz PL, Musick JA (eds) The biology of sea turtles. CRC Press, Boca Raton, FL, p 137–164

NOAA Fisheries OPR (National Oceanic and Atmospheric Administration, National Marine Fisheries Service, Office of Protected Resources) (2011) Sea turtles and the Gulf of Mexico oil spill. Accessed 23 January 2012. www.nmfs.noaa.gov/pr/health/oilspill/turtles.htm

National Research Council (2010) Assessment of sea-turtle status and trends: integrating demography and abundance. National Academies Press, Washington DC

Olgun K, Uzum N, Avci A, Miaud C (2005) Age, size, and growth of the southern crested newt *Triturus karelinii* (Strauch 1870) in a population from Bozdag (Western Turkey). Amphib-Reptilia 26:223−230

Peig J, Green AJ (2010) The paradigm of body condition: a critical reappraisal of current methods based on mass and length. Funct Ecol 24:1323−1332

Persson L (1993) Predator-mediated competition in prey refuges: the importance of habitat dependent prey resources. Oikos 68:12−22

Plotkin P (2003) Adult migrations and habitat use. In: Lutz P, Musick JA, Wyneken J (eds) The biology of sea turtles, Vol 2. CRC Press, Boca Raton, FL, p 225−242

R Development Core Team (2011) R: a language and environment for statistical computing. R Foundation for Statistical Computing, Vienna, www.R-project.org

Ramsay TO, Burnett RT, Krewski D (2003) The effect of concurvity in generalized additive models linking mortality to ambient particulate matter. Epidemiology 14:18−23

Ricker WE (1975) Computation and interpretation of biological statistics of fish populations. Bull Fish Res Board Can 191:1−382

Schauble MK (1972) Seasonal variation of newt forelimb regeneration under controlled environmental conditions. J Exp Zool 181:281−286

Schroeder BA, Owens DW (1994) Sex ratio of immature green turtles in an east central Florida developmental habitat. In: Schroeder BA, Witherington BE (compilers) Proc 13th Ann Symp Sea Turtle Biology and Conservation, NOAA Tech Memo NMFS-SEFSC-341

Schulte-Hostedde AI, Zinner B, Millar JS, Hickling GJ (2005) Restitution of mass-size residuals: validating body condition indices. Ecology 86:155−163

Schwartz FJ (1978) Behavioral and tolerance responses to cold water temperatures by three species of sea turtles (Reptilia, Cheloniidae) in North Carolina. Fla Mar Res Publ 33:16−18

Simmons DJ (1992) Circadian aspects of bone biology. In: Hall BK (ed) Bone. Bone growth — A, Vol 6. CRC Press, Boca Raton, FL, p 91−128

Snover ML, Hohn AA (2004) Validation and interpretation of annual skeletal marks in loggerhead (*Caretta caretta*) and Kemp's ridley (*Lepidochelys kempii*) sea turtles. Fish Bull 102:682−692

Snover ML, Avens L, Hohn AA (2007) Estimating growth rates in loggerhead sea turtles (*Caretta caretta*) from skeletal growth marks. Endang Species Res 3:95−104

Snover ML, Hohn AA, Goshe LR, Balazs GH (2011) Validation of annual skeletal marks in green sea turtles *Chelonia mydas* using tetracycline labeling. Aquat Biol 12: 197−204

Spotila JR, Standora EA, Morreale SJ, Ruiz GJ (1987) Temperature dependent sex determination in the green turtle (*Chelonia mydas*): effects on the sex ratio on a natural nesting beach. Herpetologica 43:74−81

Spotila JR, O'Connor MP, Paladino FV (1997) Thermal biology. In: Lutz PL, Musick JA (eds) The biology of sea turtles. CRC Press, Boca Raton, FL, p 297−314

Troëng S, Rankin E (2005) Long-term conservation efforts contribute to positive green turtle *Chelonia mydas* nesting trend at Tortuguero, Costa Rica. Biol Conserv 121: 111−116

Van Houtan KS, Hargrove SK, Balazs GH (2010) Land use, macroalgae, and a tumor-forming disease in marine turtles. PLoS ONE 5:e12900

Werner EE, Hall DJ (1988) Ontogenetic habitat shifts in bluegill: the foraging rate-predation risk trade-off. Ecology 69:1352−1366

Werner EE, Mittelbach GG, Hall DJ (1981) The role of foraging profitability and experience in habitat use by the bluegill sunfish. Ecology 62:116−125

Wibbels T (2003) Critical approaches to sex determination in sea turtles. In: Lutz P, Musick JA, Wyneken J (eds) The biology of sea turtles, Vol 2. CRC Press, Boca Raton, FL, p 103−134

Witherington BE, Ehrhart LM (1989) Hypothermic stunning and mortality of marine turtles in the Indian River Lagoon system, Florida. Copeia 1989:696−703

Wood SN (2006) Generalized additive models: an introduction with R. Chapman & Hall/CRC Press, Boca Raton, FL

Wyneken J (2001) The anatomy of sea turtles. US Dep Commer NOAA Tech Memo NMFS-SEFSC-470

Zar JH (1996) Biostatistical analysis: 3rd edn. Prentice-Hall, Englewood Cliffs, NJ

Zug GR, Glor RE (1998) Estimates of age and growth in a population of green sea turtles (*Chelonia mydas*) from the Indian River lagoon system, Florida: a skeletochronological analysis. Can J Zool 76:1497−1506

Zug GR, Parham J (1996) Age and growth in leatherback turtles, *Dermochelys coriacea* (Testudines: Dermochelyidae): a skeletochronological analysis. Chelonian Conserv Biol 2:244−249

Zug GR, Wynn AH, Ruckdeschel C (1986) Age determination of loggerhead sea turtles, *Caretta caretta*, by incremental growth marks in the skeleton. Smithson Contrib Zool 427:1−34